Early diagenetic vivianite [Fe-3(PO4)(2) center dot 8H(2)O] in a contaminated freshwater sediment and insights into zinc uptake: a mu-EXAFS, mu-XANES and Raman study

Early diagenetic vivianite ($Fe_3(PO_4)_2.8H_2O$) from contaminated freshwater sediments: a μ-EXAFS, μ-XANES and μ-Raman study

Kevin G. Taylor[1]*, Karen A. Hudson-Edwards[2], Andrew J. Bennett[3] and Vladimir Vishnyakov[4]

[1] Department of Environmental and Geographical Sciences, Manchester Metropolitan University, Chester Street, Manchester, M1 5GD, U.K.

[2] School of Earth Sciences, Birkbeck, University of London, Malet Street, London WC1E 7HX, U.K.

[3] SRS Daresbury Laboratory, Warrington, Cheshire, WA4 4AD, U.K.

[4] School of Biology, Chemistry and Health Sciences, Manchester Metropolitan University, Chester Street, Manchester, M1 5GD, U.K.

* Corresponding author. E-mail: k.g.taylor@mmu.ac.uk

Abstract

The sediments in the Salford Quays, a heavily-modified urban water body, contain high levels of organic matter, iron, zinc and nutrients as a result of past contaminant inputs. Vivianite [$Fe_3(PO_4)_2.8H_2O$] has been observed to have precipitated within these sediments during early diagenesis as a result of the release of Fe and P to porewaters. These mineral grains are small (<100

μm) and micron-scale analysis techniques (SEM, electron microprobe, μ-EXAFS, μ-XANES and μ-Raman) have been applied in this study to obtain information upon the structure of this vivianite and the nature of Zn uptake in the mineral. Petrographic observations, and elemental, X-ray diffraction and Raman spectroscopic analysis confirms the presence of vivianite. EXAFS model fitting of the Fe K-edge spectra for individual vivianite grains produces Fe-O and Fe-P co-ordination numbers and bond lengths consistent with previous structural studies of vivianite (4 O atoms at 1.99-2.05 Å; 2 P atoms at 3.17-3.25 Å). One analysed grain displays evidence of a significant Fe^{3+} component, which we interpret to have resulted from oxidation during sample handling and/or analysis. EXAFS modelling of the Zn K-edge data, together with linear combination XANES fitting of model compounds, indicates that Zn may be incorporated into the crystal structure of vivianite (4 O atoms at 1.97 Å; 2 P atoms at 3.17 Å). Low levels of Zn sulphate or Zn-sorbed goethite are also indicated from linear combination XANES fitting and to a limited extent, the EXAFS fitting, the origin of which may either be an oxidation artifact or the inclusion of Zn sulphate into the vivianite grains during precipitation. This study confirms that early diagenetic vivianite may act as a sink for Zn, and potentially other contaminants (e.g. As) during its formation and, therefore, forms an important component of metal cycling in contaminated sediments and waters. Furthermore, for the case of Zn, our EXAFS fits for Zn phosphate suggest this uptake is structural and not via surface adsorption.

1. Introduction

The cycling of contaminant elements and nutrients between freshwater lake sediments and waters plays a key role in the chemical and ecological functioning of these important environments. It has long been known that early diagenesis plays a particularly strong role in the short- to long-term release of the chemical species Fe, Mn, contaminant elements and P (Hamilton-Taylor et al., 1996a, b; Bryant et al., 1997; Taylor et al., 2003). The release of P from sediments during early diagenesis

has been recognised to be an important control on water quality in freshwater systems (Carignan and Flett, 1981; Jensen et al., 1992; Hupfer et al., 1995; Gonsiorczyk et al., 2001).

As diagenesis proceeds, a build up of porewater solutes may lead to mineral saturation, resulting in the precipitation of authigenic sulphides, carbonates and phosphates. These precipitates may also sorb or co-precipitate trace metals, thereby acting as long-term sinks for contaminants in sediments. For example, early diagenetic sulphides in marine sediments have been shown to act as sinks for the metallic elements Cu, Pb and Zn (Ankley et al., 1996; Parkman et al., 1996; Pirrie et al., 1999). The absence of significant sulphate reduction in freshwaters has led to the assumption that such sinks do not exist in freshwater sediments. It is known, however, that the iron phosphate mineral vivianite [$Fe_3(PO_4)_2.8H_2O$] may precipitate during early diagenesis in freshwater sediments (Nriagu and Dell, 1974; Emerson and Widmer, 1978), and it has recently been documented that vivianite can be abundant in nutrient-rich freshwater sediments (Dodd et al., 2000; Taylor and Boult, 2007). These sediments result from inputs from sewage-treatment works and from fertilizer runoff from land, and are therefore of considerable concern. Vivianite is the Fe-rich end-member of the vivianite mineral group [$X_3(YO_4)_2 \cdot 8H_2O$, where X=Co, Fe, Mg, Mn, Ni or Zn, and Y=P or As]. It should theoretically be possible for vivianite to co-precipitate or sorb substantial amounts of the contaminant elements Mn, Ni, Zn, Co and As, and the nutrient P. Since no quantitative data have been collected on the partitioning of contaminants into vivianite during early diagenesis, nor the mechanisms by which this takes places, the aim of this study was to test the hypothesis that naturally-occurring vivianite is a significant sink for contaminant elements (in this case Zn) in a contaminated freshwater sediment.

2. Study Site

Vivianite analysed in this study is a diagenetic mineral present in the heavily contaminated Salford Quays of the Manchester Ship Canal, Manchester, NW England (Fig. 1). A full description of this site,

and its contamination and remediation history, can be found in Taylor et al. (2003). The Manchester Ship Canal is up to 8 m deep, steep-sided and up to 50 m wide. As a result, flow is slow, and this has led to the accumulation of highly contaminated, organic-rich sediments. Although the site has recently been significantly remediated as regards to contaminant inputs, the historical sediments present in the Quays are metal-rich, containing maximum concentrations of Zn, Cu and Pb of 30,000 μg/g, 7000 μg/g, and 4000 μg/g, respectively, and Fe, Mn, Zn and P are present in porewaters at concentrations up to 700 μM, 50 μM and 2 μM, respectively. Taylor and Boult (2007) documented the presence of Zn-rich glass grains in these sediments, which are undergoing diagenetic dissolution. They also documented the precipitation of vivianite in these sediments within the first few cm of the sediment-water interface, and suggested that this mineral may play an important role in contaminant metal cycling at the site, but did not determine any chemical or structural data for it.

3. Experimental and Materials

Sediment cores were taken from Basin 9 of the Salford Quays (Fig. 1) using a 1 m long, 60 mm diameter stainless steel corer with a stainless steel liner. The corer was pushed into the sediment using lengths of steel rod, and the core retrieved. The collected core was split into 1 cm vertical sub-sections by use of a screw-threaded plunger, in a N_2-filled glove-bag to minimise oxidation of reduced species, and samples placed into acid-washed, N_2-purged centrifuge tubes and sealed. Porewater separation and analysis of these sediments is reported in Taylor & Boult (2007).

The sediment mineralogy was characterised by whole rock X-ray diffraction (XRD) analysis of N_2-dried powdered samples. Samples were run on a Philips PW1050 X-ray diffractometer, using CuKα radiation, with scans taken from 4º to 64º at a scan rate of 2º/min. Petrographic and quantitative chemical data were obtained through the use of scanning electron microscopy (SEM) and electron

microprobe analysis. N_2-dried samples of sediment were impregnated with epoxy resin and polished surface blocks produced. These blocks were analysed using a JEOL 5600LV SEM, operating at 15kV and with a working distance of 15 mm, using backscattered electron (BSE) imagery. A Link eXL energy dispersive X-ray microanalysis system (EDX) was used to obtain semi-quantitative data on major element compositions of mineral grains. Fully quantitative chemical data for both major and trace elements were obtained using wavelength-dispersive X-ray analysis on a Cameca SX100 electron microprobe. Detection limits for trace metals using this technique is on the order of 100 ppm.

X-ray absorption near-edge structure (XANES) and extended X-ray absorption fine structure (EXAFS) spectroscopies were used to investigate how Fe and Zn are bound within the vivianites. Reviews of the principles of these methods and mineral systems applications can be found in Calas et al. (1984) and Brown et al. (1988). For this study, X-ray absorption spectra at the Cu and Fe K-edges and Pb LIII-edge were collected at the minifocus XAS Station 9.2 at the Synchrotron Radiation Source (SRS) at Daresbury Laboratory, UK. The storage ring operated at 2 GeV with a current of between 125 and 250mA. Spectra were collected using a water-cooled, double crystal Si111 monochromator detuned 70% to remove high energy harmonics. Two Kirkpatrick-Baez mirrors (substrate ULE glass coated with 15 nm Rh on 20 nm Pt) are used to focus the beam horizontally and vertically to a spot size of ~50 µm. Stability of the focussed beam is less than the spot size. For fluorescence measurements a Canberra 13-element solid state Ge detector with full electronics including semi-automatic windowing was used. For both the natural and synthetic samples, encased in polished epoxy blocks, an XRF map of the elements of interest (Fe, Zn) was collected using GDA Acquisition Version 5.6.0 software. “Hotspots”, where concentrations of the respective element were high, were selected from the XRF map for further analysis by XAS. Between 6 and 16 XAS scans were collected for each element for each of the “hotspots”. Incident and transmitted intensities were measured using ionisation chambers filled with a He/Ar mix appropriate for the X-ray energy of interest. X-ray absorption spectra were collected in

fluorescence mode (16 scans) for both the Fe K-edge and Zn K-edge for four vivianite grains previously characterized by SEM and electron microprobe. X-ray absorption spectra were also collected in transmission mode (single scan) at the Zn K-edge for a suite of Zn model compounds (Zn metal foil, $Zn_3(PO_4)_2$, $ZnNO_3$, $ZnCO_3$, ZnS_2, $ZnSO_4$, ZnO, Zn-sorbed goethite) to allow comparison with experimental data for the natural samples. With the exception of Zn-sorbed goethite, the model compounds were chemical standards of 98% purity or greater. Goethite was synthesized in the laboratory according to the methods of Schwertmann and Cornell (1991), and Zn sorbed to it using the methods of Parkman et al. (1999).

Comment [khe1]: Do you mean ZnS here?

The X-ray absorption spectra of the Zn and Fe K-edges were measured. Data were collected from ~200 eV before to ~600 eV above the standard edge position. In the pre-edge region the X-ray energy step size was large (~9 eV), across the edge the step size was 0.6-1 eV and in the post edge region the step size was 1.5-2 eV. The spectra were processed using the computer programs EXCALIB, EXBROOK, EXSPLINE and EXCURV98 compiled at the SRS (Binsted, 1998). The spectra were summed using the EXCALIB program. This process also converted the monochromator angle into X-ray energy.

For XANES analysis the edge position was determined and the data normalised such that the edge step was equal to one using the EXBROOK program. Linear combination fitting was performed on the XANES portion of the data using the model compounds stated above. The proportion that each of these standards in the spectra and a least squares residual factor were calculated. These standards were measured for XANES and EXAFS comparisons.

For analysis of the EXAFS oscillations, the background was subtracted from the raw XAS spectra and the data normalised using the EXSPLINE program. A spline curve, which estimates the smooth background absorbance, was used to remove the smooth background absorbance. No more than 3

spline points were used. The data were then normalised so that the edge step is equal to one. The energy range of the spectrum was reduced if there was significant noise present in the higher energy region of the spectra. The EXAFS spectrum was then weighted by k^3 to amplify the upper k range. The final step was the Fourier Transform (FT) of the data in order to convert energy into a radial distribution function over a k range of 2 to 13 $Å^{-1}$.

Once the EXAFS and the FT had been calculated the data were fitted to gain structural information. EXCURV98 (Binstead, 1998; Rehr & Albers, 1990) used exact curved wave theory (Lee & Pendry, 1975) to simulate EXAFS. The element, coordination number (CN), distance and Debeye-Waller factor were determined using this phase and amplitude functions from this program. Standard compound EXAFS traces were also used to compare with experimental samples in order to determine similarities in the spectra. Single and multiple scattering were considered however multiple scattering did not improve the fit for any sample. During fitting the Eo value, distance, Debeye-Waller factor and CN were varied. Identification of possible elements was determined by differences in the amplitude and phase and possible structural configurations taken from databases, e.g. Inorganic Chemical Structural Database (www.cds.dl.ac.uk/icsd). The accuracy of the fit was determined using the R factor statistical parameter for which a lower value indicates a better fit. The fitting procedure accurately determines distances to within 0.02 Å, but coordination number is highly correlated to the Debeye-Waller factor and hence larger errors (±1) exist.

For Raman microprobe spectroscopy grains of vivianite were analysed, using the same polished blocks as for SEM and XAS, on a Renishaw 1000 Raman microscope system at Manchester Metropolitan University. The samples were placed, and areas of analysis located, on the stage of a Leica microscope, with 10, 20 and 50× objective lens. Measurements were made at room temperature using a 514 nm laser argon at 10% power, and the laser spot size was less than 5 μm. Multiple (five) acquisitions were

made to maximize the noise-to-signal ratio. Spectra were also collected for a natural, hydrothermal crystalline sample of vivianite from Bolivia.

Comment [khe2]: Do we have any more information about where in Bolivia / which ore deposit / this sample came from?

4. Results and Discussion

4.1 Mineralogy of the vivianite grains

The presence of vivianite [$Fe_3(PO_4)_2.8H_2O$] was confirmed by comparing the powder XRD patterns to the those reported for vivianite in the Mincryst mineral structural CPDS files. (Fig. 2). No quantitative measures of vivianite abundances were made, but the presence of significant XRD peaks for vivianite suggests that levels in the sediment are in excess of 1%.

The abundance of vivianite was confirmed by SEM observations of the bulk sediment. Backscatter electron SEM imaging shows that the vivianites are radiating lath-shaped crystals and needle-like masses growing within the sediment matrix (Fig. 3). Electron microprobe analyses for the vivianite grains have been published previously (full details can be found in Taylor and Boult, 2007). The vivianite crystals contain significant amounts of Mn (up to 5.4% MnO) and contain up to 550 μg/g of Zn.

The classification of the grains as vivianite was also supported by Raman spectroscopy. A typical Raman spectra for the Salford Quays vivianite grains is shown in figure 4, together with the spectra of a well-characterised crystalline vivianite. In both cases, the bands are in good agreement. The major band at 950 cm^{-1} has been assigned to the Raman active P-O stretching vibration, and bands at 1050 cm^{-1} and 1020 cm^{-1} are similar to those assigned to the P-O anti-symmetric stretching vibration (Pirrou and Poullen, 1987; Frost et al., 2002, 2003). The bands at 230 cm^{-1} and 175 cm^{-1} are reported in vivianite (Frost et al., 2002, 2003) and may be attributed to the Fe-O stretching vibration. The bands

associated with the 550 cm^{-1} peak are attributed to the ν_4 modes, and the band at 460 cm^{-1}, to the ν_2 mode of the phosphate ion, respectively (Frost et al., 2002, 2003).

4.2. Speciation and bonding environment of Fe in vivianite grains

Nriagu (1972) has pointed out that poorly-crystalline, redox-sensitive phases such as vivianite are prone to oxidation when exposed to standard laboratory conditions. The XRD, SEM and Raman data presented above suggest that oxidation of the Salford Quays vivianite grains is limited. This is confirmed by Fe K-edge XANES spectra for the vivianite grains 2 to 4 (Figure 5). However, for the vivianite 1 grain, a shift in the Fe K-edge and details in the pre-edge area, suggests significant amounts of Fe^{3+}. The smaller features on the pre-edge area of grains 2 to 4, with different edge position to that in grain 1, are consistent with an Fe^{2+} pre-edge feature.

The parameters derived from the EXAFS fitting for Fe are shown in Table 1, together with Fe-O and Fe-P co-ordination numbers and bond lengths for vivianite from Mori and Ito (1950), Fejdi et al. (1980) and Bartl (1989). EXAFS Fe K-edge spectra and Fourier transforms for vivianites 1 and 4 are shown in Figure 6 (the spectra for vivianites 2 and 3 are virtually identical to that of vivianite 4 and so are not shown). The results from a first shell fitting for the apparently unoxidised vivianites (2 to 4) suggest that Fe exists in tetrahedral coordination, with Fe-O distances of 2.03-2.05 Å. Crystallographic studies of vivianite suggest that Fe occupies two distinct octahedral sites, with $Fe_2O_6(H_2O)_4$ groups linked to two neighbouring similar groups and to four other single octahedral groups, $FeO_2(H_2O)_4$, by P (Mori and Ito, 1950; Fejdi et al., 1980; Bartl, 1989; Table 1). Because it is an averaging technique, the EXAFS analysis is unable to resolve these differences in our vivianites, but the bond distance of 2.03-2.05 Å is similar to the average first shell Fe-O distances calculated for the data of Fejdi et al. (1980) and Bartl (1989; Table 1) and the average second shell distance of 2.02 Å calculated for the data of Mori and Ito (1950). The tetrahedral coordination fit for our vivianites also matches the second shell of these previous studies, suggesting that either our data are not of sufficient quality to fit the additional

shell of 2 O around the Fe, or that the Fe is more disordered within the normally octahedral site. The identification of a shell of two P atoms at a distance of 3.23 Å in grains 2 to 4 is typical of the vivianite structure (Mori and Ito, 1950; Fejdi et al., 1980; Bartl, 1989; Table 1).

First and second shell fits for the apparently oxidized vivianite 1 grain are similar to those of vivianites 2 to 4 in terms of the scatterer atoms and their co-ordination, but bond distances are slightly shorter (O – 1.99 Å; P – 3.17 Å; Table 1). This is likely due to the formation of an FeIII phase.

4.3. Bonding environment of Zn in vivianite grains

The Zn K-Edge XANES data for the vivianite grains, along with those for model compounds, are shown in Figure 7. Parameters from the Zn EXAFS fitting for vivianites 2 and 3 (the only two grains with clean enough spectra for fitting) are shown in Table 1, and the K-edge EXAFS spectra and Phase Shifted Fourier transforms in Figure 8.

XANES linear combination fitting for the apparently unoxidised (or very minimally oxidised) grains 2 to 4 suggest 85% phosphate or Zn-sorbed goethite (the XANES for these are almost identical) and 15% Zn sulphate (errors in linear combination fitting are +/- 10%). EXAFS fits for grain 2 define three shells of atoms around the Zn: a first shell of 4 O at 1.97 Å, a second shell of 2 O at 2.98 Å, and a third shell of 2 O at 3.17 Å. The first and third shells exactly match O and P distances and coordination numbers reported for Zn phosphate dehydrate by Sarrett et al. (2001). This, together with the XANES fitting, suggests that Zn may be substituting for Fe in the vivianite structure. The shorter first shell O distance for Zn compared to Fe (Table 1) may be due to the larger ionic radius of the former.

The first shell of 4 O atoms fit for Zn also matches that of a first shell fitting of Zn sorbed on goethite (Trivedi et al., 2001). This, together with the XANES fitting and the small amount of FeIII in grain 2 (see above), suggest that some Zn-sorbed goethite may be present. However, Trivedi et al. (2001) also report a second shell of 1.74 to 2.89 Fe atoms with Zn-Fe distances of 3.51-3.54 Å, which

do not match any of our calculated distances (Table 1), suggesting that, if present, the amounts of Zn-sorbed goethite in our samples are small.

The second shell of O atoms at 2.98 Å fit for grain 2 is unlike any previously reported distances for metal-O bonds in vivianites, or for Zn sorbed to goethite (Table 1; Trivedi et al., 2001). Given the XANES fitting, it is possible that this second shell fit is indicative of Zn sulphate either within, or sorbed on, the vivianite structure. Sulphate is known to substitute for phosphate in other minerals (e.g., orpheite $PbAl_3(PO_4,SO_4)_2(OH)_6$), and moderate concentrations of SO_4^{2-} are reported in Salford Quays porewaters (Taylor and Boult, 2007). If true, then the amounts of Zn sulphate substituting in the structure are probably very low, given that no bands attributable to sulphate (ν_1 983, ν_2 450, ν_3 1105 and ν_4 611 cm^{-1}; Ross, 1974) are recorded in the Raman spectra (Figure 4). The Zn sulphate may therefore be forming post-vivianite formation, possibly during oxidation of the grain. Despite all of this, the bond distance of 2.98 Å does not match any Zn-O distances reported for the Zn sulphate mineral zincosite (2.312, 2.113, 1.970 Å; Wildner and Giester, 1988). It is therefore possible that the 2.98 Å bond distance represents an average of different Zn bond types including sulphate or Zn sorbed to goethite, as above. (Figure 5).

For grain 3, only one shell of 4 O at 1.97 Å was fit around Zn. This is identical to the first shell fit for grain 2, but in this case the lack of extra shells suggests less long-range order (due to either lower concentration of Zn or fewer scans collected) and possibly sorption of Zn on the vivianite surface rather than incorporation within the structure. As with grain 2, the fit of 4 O at 1.97 Å also matches that of Zn-sorbed goethite (Trivedi et al., 2001), and this, together with the possible presence of FeIII, suggests that Zn-sorbed goethite may also be present.

For the apparently oxidised grain 1, linear combination XANES fitting yielded 42% Zn goethite or phosphate, and 58% Zn sulphate. This may be indicative of secondary Zn sulphate or Zn-sorbed

goethite formation following oxidation of this grain. As with grain 2, this may indicate the presence of structural Zn phosphate and sulphate, as well as secondary Zn sulphate and Zn-sorbed goethite.

5. Implications

The study has shown that the use of μ-Raman and μ-XAS analysis of low temperature mineral precipitates in sediment systems can provide critical information upon the structure and composition of these minerals. Given that low temperature diagenetic minerals are commonly fine-grained and poorly crystalline, the application of these techniques promises to provide new insights into the mechanisms of precipitation and nature of these important minerals. We have shown for the first time that Zn may be incorporated into the crystal structure of vivianite. These findings indicate that vivianite can indeed act as a significant sink for trace metals in contaminated sediments during early diagenesis. Early diagenetic sulphide mineral precipitates have been documented previously to act as sinks for trace metals in marine and brackish sediments (Parkman et al., 1996; Pirrie et al., 1999; Morse and Luther, 1999) and these minerals are routinely considered in contaminated marine sediment assessment (Ankley et al., 1996). Our study is the first to consider the incorporation of the potentially toxic element Zn in vivianite, an important mineral in anoxic environments such as acid mine drainage sites (Ueshima et al., 2004), rivers (House, 2003), lakes (Fagel et al., 2005) and urban water bodies (Taylor et al., 2003). There is a need to study the role of vivianite in the uptake of other potentially toxic elements in freshwater systems (e.g. As, Pb, Sb).

6. Conclusions

1) Petrographic observations, and elemental, X-ray diffraction and Raman spectroscopic analysis confirms the presence of vivianite [$Fe_3(PO_4)_2.8H_2O$], precipitated during early diagenesis, within the sediments of the urban water body of the Salford Quays, Greater Manchester, NW England.

2) EXAFS model fitting of the Fe K-edge spectra for individual vivianite grains produces Fe-O and Fe-P co-ordination numbers and bond lengths consistent with previous structural studies of vivianite. One analysed grains displays evidence for the presence of a significant Fe^{3+} component, which we interpret to have resulted from oxidation during sample handling and/or analysis.

3) EXAFS modelling of the Zn K-edge data, together with linear combination XANES fitting of model compounds, indicates that Zn may be incorporated into the vivianite as a Zn-phosphate structure. Low levels of Zn sulphate or Zn-sorbed goethite are also indicated from linear combination XANES fitting and to a limited extent, the EXAFS fitting, the origin of which may either be an oxidation artifact or the inclusion of Zn sulphate into the vivianite grains during precipitation.

4) This study confirms that early diagenetic vivianite may act as a sink for contaminant metals during its formation and, therefore, forms an important component of metal cycling in contaminated sediments and waters. Furthermore, for the case of Zn, our data suggest that this uptake is structural and not surface adsorption. This observation highlights the need to consider the role of vivianite in the uptake of other potentially toxic elements in freshwater systems (e.g. As).

Acknowledgements

This research was funded by the UK Natural Environment Research Council (Grant GST/02/2255) and the UK CCLRC Daresbury Laboratory (provision of beamtime through direct access award 45/241). David Plant, University of Manchester, is thanked for help with the electron microprobe analysis and

for providing the crystalline vivianite sample. We would like to thank Natalie Fagel for constructive comments on an earlier version of the manuscript.

References

Ankley, G.T., Di Toro, D.M., Hansen, D.J., Berry, W.J., 1996. Technical basis and proposal for deriving sediment quality criteria for metals. Environ. Toxicol. Chem. 15, 2056-2066.

Bartl, H., 1989. Water of crystallization and its hydrogen-bonded cross linking in vivianite $Fe_3(PO_4)_2 \cdot 8H_2O$: a neutron diffraction investigation. Fresenius' Zeitschrift Fuer Analytische Chemie. 333, 401-403.

Bryant, C.L., Farmer, J.G., MacKenzie, A.B., Bailey-Watts, A.E., Kirika, A., 1997. Manganese behaviour in the sediments of diverse Scottish freshwater lochs. Limnol. Oceanog. 42, 918-929.

Binsted, N. (1998) EXCURV98 Program. Daresbury Laboratory, UK.

Brown, G.E.Jr., Calas, G., Waychunas, G.A., Petiau, J., 1988. X-ray absorption spectroscopy and its applications in mineralogy and geochemistry. Rev. Mineral. 18, 431-512.

Calas, B., Bassett, W.A., Petiau, J., Steniberg, M., Tchonbar, D., Zarka, A., 1984. Some mineralogical applications of synchrotron radiation. Phys. Chem. Min. 11, 17-36.

Carignan, R., Flett, R.J., 1981. Post-depositional mobility of phosphorus in lake-sediments. Limnol. Oceanog. 26, 361-366.

Dodd, J. Large, D.J., Fortey, N.J., Milodowski, A.E., Kemp, S., 2000. A petrographic investigation of two sequential extraction techniques applied to anaerobic canal bed mud. Environ. Geochem. Health 22, 281-296.

Emerson, S., Widmer, G., 1978. Early diagenesis in anaerobic lake sediments – II. Thermodynamic and kinetic factors controlling the formation of iron phosphate. Geochim. Cosmochim. Acta 42, 1307-1316.

Fagel, N., Alleman, L.Y., Granina, L., Hatert, F., Thamo-Bozso, E., Cloots, R., André, L., 2005. Vivianite formation and distribution in Lake Baikal sediments. Glob. Planet. Change, 46, 315-336.

Fejdi, P., Poullen, J.F., Gasperin, M., 1980. Affinement de la structure de la vivianite $Fe_3(PO_4)_2(H_2O)_8$. Bull. Mineralogie 103, 135-138.

Frost, R.L., Kloprogge, T., Weier, M.L., Wayde, W.N., Ding, Z., Edwards, G.H., 2003. Raman spectroscopy of selected arsenates – implications for soil remediation. Spectrochim. Acta Part A 59, 2241-2246.

Frost, R.L., Martens, W., Williams, P.A., Kloprogge, J.T., 2002. Raman and infrared spectroscopic study of the vivianite-group phosphates vivianite, baricite and bobierrite. Min. Mag. 66, 1063-1073.

Gonsiorczyk, T., Casper, P., Koschel, R., 2001. Mechanisms of phosphorus release from the bottom sediment of the oligotrophic Lake Stechlin: importance of the permanently oxic sediment surface. Arch. Hydrobiol. 151, 203-219.

Hamilton-Taylor, J., Davison, W., Morfett, K., 1996a. The biogeochemical cycling of Zn, Cu, Fe, Mn and dissolved organic C in a seasonally anoxic lake. Limnol. Oceanogr. 41, 408-418.

Hamilton-Taylor, J., Davison, W., Morfett, K., 1996b. A laboratory study of the biogeochemical cycling of Fe, Mn, Zn and Cu across the sediment-water interface of a productive lake. Aquat. Sci. 58, 191-209.

House, W.A., 2003. Geochemical cycling of phosphorus in rivers. Appl. Geochem. 18, 739-748

Hupfer, M., Gachter, R., Giovanoli, R., 1995. Transformation of phosphorus species in settling seston and during early sediment diagenesis. Aquat. Sci. 57, 305-324.

Jensen, H.S., Kristensen, P., Jeppesen, E., Skytthe, A., 1992. Iron-phosphorus ratio in surface sediment as an indicator of phosphate release from aerobic sediments in shallow lakes. Hydrobiol. 235, 731-743.

Lee, P.A, Pendry, J.B., 1975. Theory of the extended x-ray absorption fine structure. Phys. Rev. B 11, 2795-2811.

Mori, H., Ito T., 1950. The structure of vivianite and symplesite. Acta Cryst. 3, 1-6.

Morse, J.W., Luther, G.W., 1999. Chemical influences on trace metal-sulfide interactions in anoxic sediments: Geochim. Cosmochim. Acta 63, 3373-3378.

Nriagu, J.O., 1972. Stability of vivianite and ion-pair formation in system $Fe_3(PO_4)_2$-H_3PO_4-H_2O. Geochim. Cosmochim. Acta 36, 459 -470.

Nriagu, J.O., Dell, C.I., 1974. Diagenetic formation of iron phosphates in recent lake sediments. Am. Mineral. 59, 934-946.

Parkman, R.H., Curtis, C.D., Vaughan, D.J., Charnock, J.M., 1996. Metal fixation and mobilization in the sediments of Afon Goch Estuary, Dulas Bay, Anglesey. Appl. Geochem. 11, 203-210.

Parkman, R.H., Charnock, J.M., Bryan, N.D., Livens, F.R., Vaughan, D.J., 1999. Reactions of copper and cadmium ions in aqueous solution with goethite, lepidocrocite, mackinawite, and pyrite. Am. Mineral. 84, 407-419.

Piriou, B., Poullen, J.F., 1987. Infra-red study of the vibrational modes of water in vivianite. Bull. Mineralogi 110, 697

Pirrie, D., Beer, A.J., Camm, G.S., 1999. Early diagenetic sulphide minerals in the Hayle Estuary, Cornwall. Geoscience in Southwest England 9, 325-332.

Rehr, J.J., Albers, R.C., 1990. Scattering-matrix formulation of curved-wave multiple-scattering theory: application to x-ray absorption fine structure. Phys. Rev. B 41, 8139 - 8149

Ross, S.D., 1974. The Infrared Spectra of Minerals. The Mineralogical Society, London, 423 pp. (Chapter 18).

Sarret, G., Vangronsveld, J., Manceau, A., Musso, M., D'haen, J., Menthonnex, J.-J., Hazemann, J.-L., 2001. Accumulation forms of Zn and Pb in Phaseolus vulgaris in the presence and absence of EDTA. Environ. Sci. Technol. 35, 2854-2859.

Schwertmann, U., Cornell, R.M., 1991. Iron oxides in the laboratory: preparation and characterization. VCH Publishers, New York, 137 p.

Taylor, K.G. and Boult, 2007 (in press) The role of grain dissolution and diagenetic mineral precipitation in the cycling of metals and phosphorus: a study of a contaminated urban freshwater sediment. Appl. Geochem.

Taylor, K.G., Boyd, N.A., Boult, S., 2003. Sediments, porewaters and diagenesis in an urban water body, Salford, UK: impacts of remediation. Hydrol. Processes 17, 2049-2061.

Trivedi, P., Axe, L., Tyson, T.A., 2001. An analysis of zinc sorption to amorphous versus crystalline iron oxides using XAS. J. Colloid Interface Sci. 244, 230-238.

Ueshima, M., Fortin, D., Kalin, M., 2004. Development of iron-phosphate biofilms on pyretic mine waste rock surfaces previously treated with natural phosphate rocks. Geomicrobiology J. 21, 313-323.

Wildner, M., Giester, G. 1988. Crystal structure refinements of synthetic chalcocyanite ($CuSO_4$) and zincosite ($ZnSO_4$). Mineral. Petrol. 39, 201-209.

Figure Captions

Figure 1 – Location map of the Salford Quays and the Manchester Ship Canal, showing the location of the sediment core samples.

Figure 2 – A typical X-ray diffractogram of a sample of sediment from the Salford Quays (this sample from 10cm below the sediment surface). The vivianite peaks are marked (V), with the calculated d-spacings (in angstroms). Other mineral peaks are marked (Q = quartz; M = mica; K = kaolinite; C = calcite).

Figure 3 – Backscatter electron images of the vivianite grains analysed by Raman and XAS in this study. The black areas surrounding the grains are resin.

Figure 4 - Raman spectra of one of the vivianite grains (vivianite 2), together with the spectra for a crystalline vivianite sample of hydrothermal origin, Bolivia.

Figure 5 – Normalised Fe XANES for vivianite grains 1 to 4.

Figure 6 –Normalised Fe K-edge EXAFS and Phase Shifted Fourier Transform spectra for vivianites 1 to 4. Dashed lines are least-squares fits using parameters shown in Table 1.

Figure 7 – Normalised Zn XANES for vivianite grains 1 to 4, and for model compounds.

Figure 8 – Normalised Zn K-edge EXAFS and Phase Shifted Fourier Transform spectra for vivianites 2 and 3. Dashed lines are least-squares fits using parameters shown in Table 1.

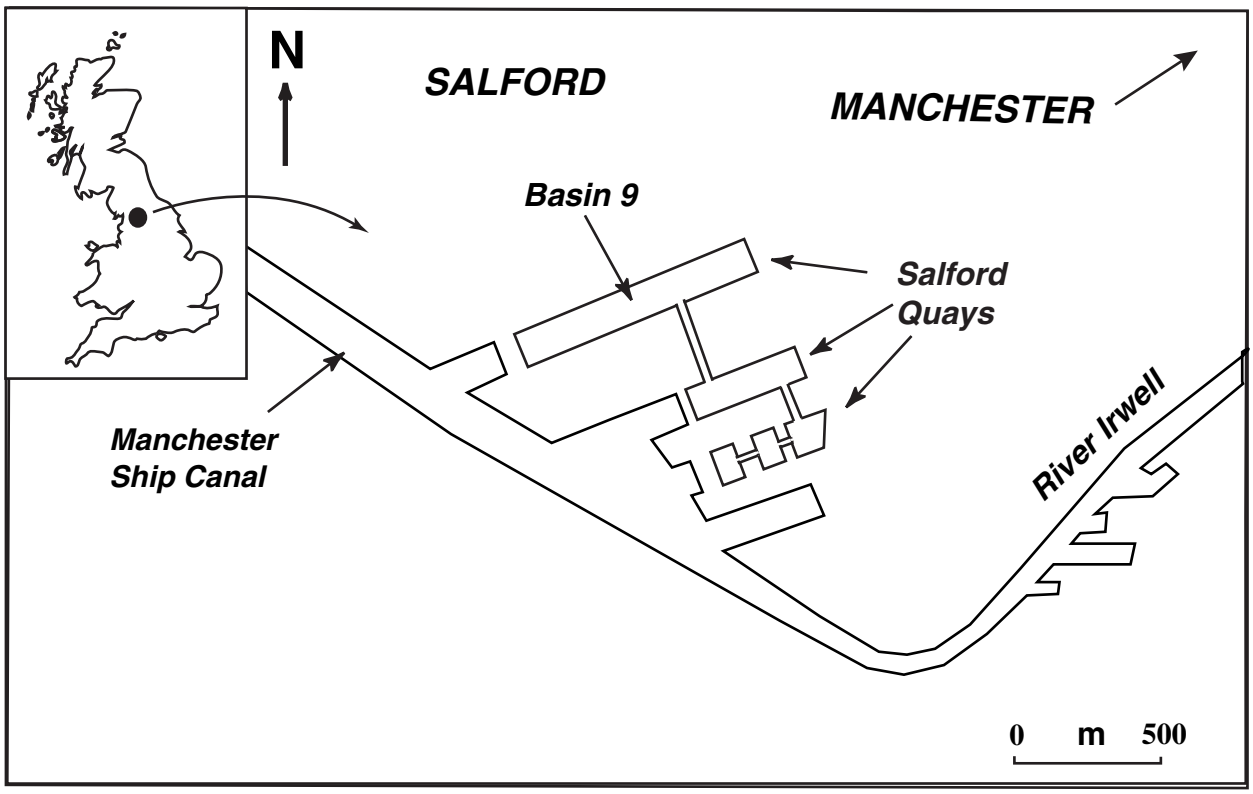
N
SALFORD
MANCHESTER
Basin 9
Salford
Quays
Manchester
Ship Canal
River Irwell
0 m 500

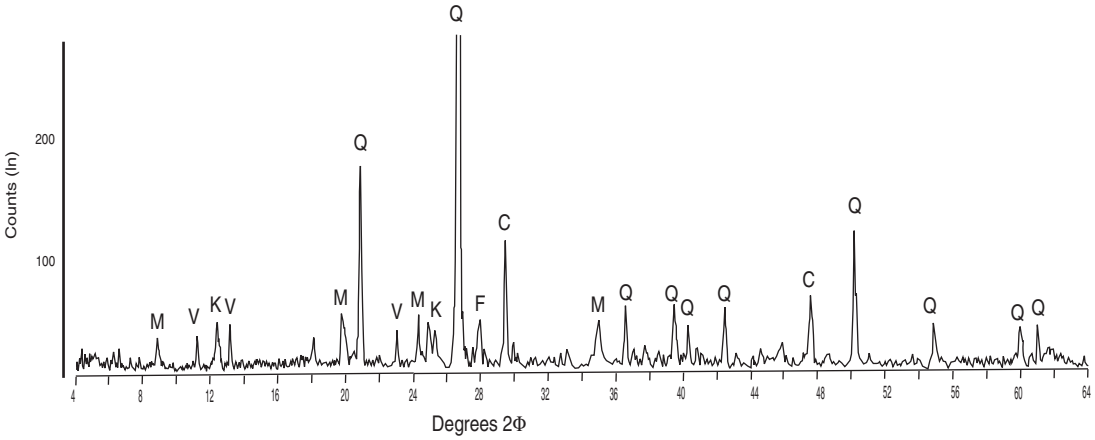
Counts (In)
200
100
Q
Q
C
Q
M
V
K V
M
V
M
K
F
M
Q
Q Q
Q
C
Q
Q
Q Q
4
8
12
16
20
24
28
32
36
40
44
48
52
56
60
64
Degrees 2Φ

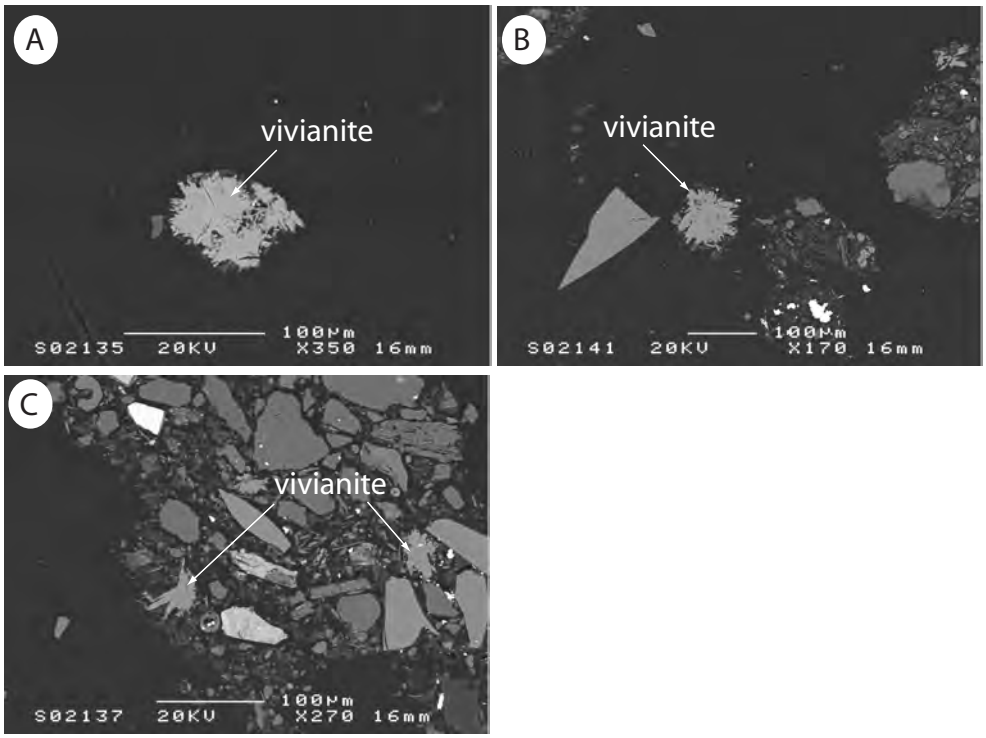
A
vivianite
100µm
S02135 20KV X350 16mm
B
vivianite
100µm
S02141 20KV X170 16mm
C
vivianite
100µm
S02137 20KV X270 16mm

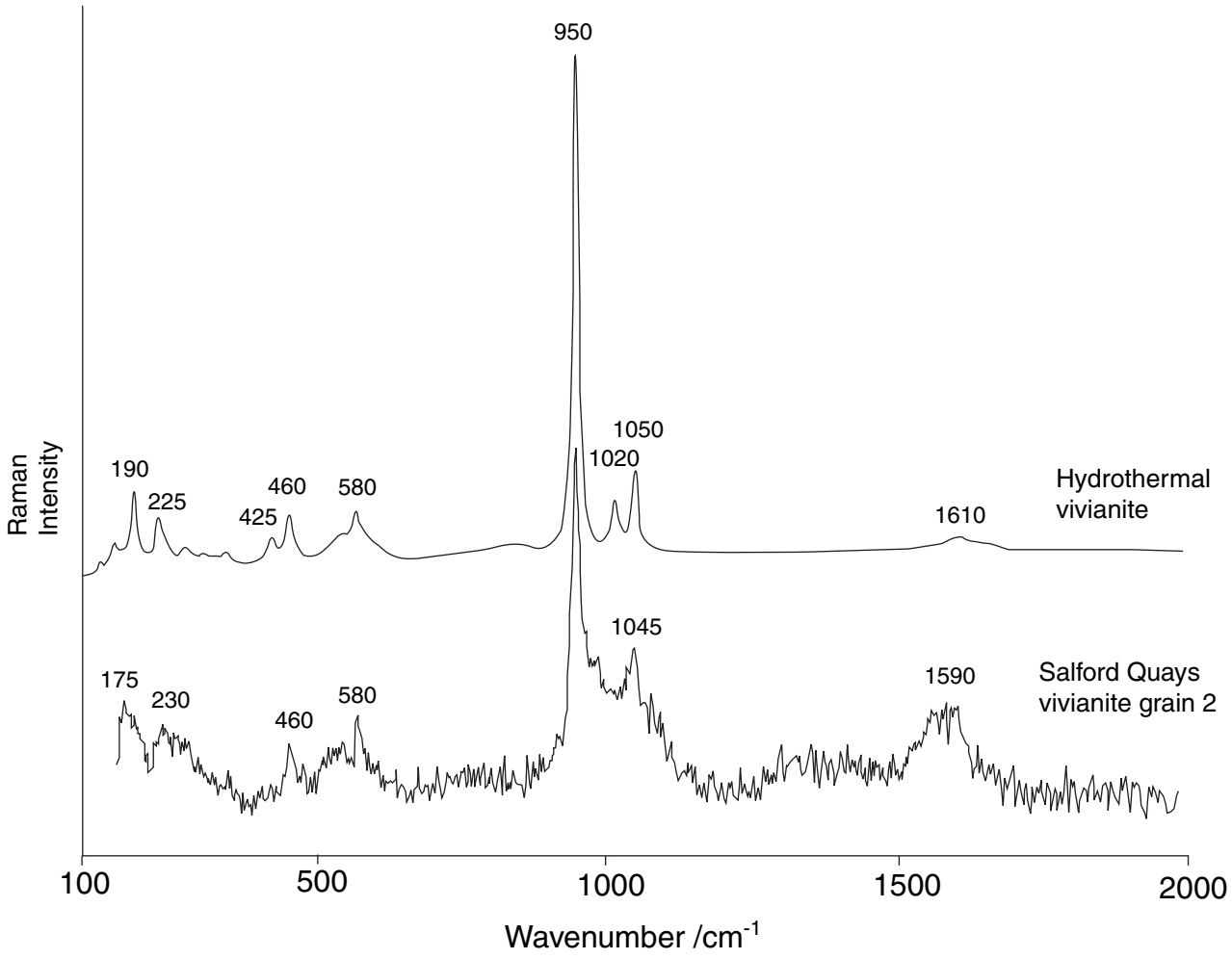
950
1050
1020
190
225
425
460
580
1610
Hydrothermal
vivianite
1045
175
230
460
580
1590
Salford Quays
vivianite grain 2
Raman
Intensity
100
500
1000
1500
2000
Wavenumber /cm-1

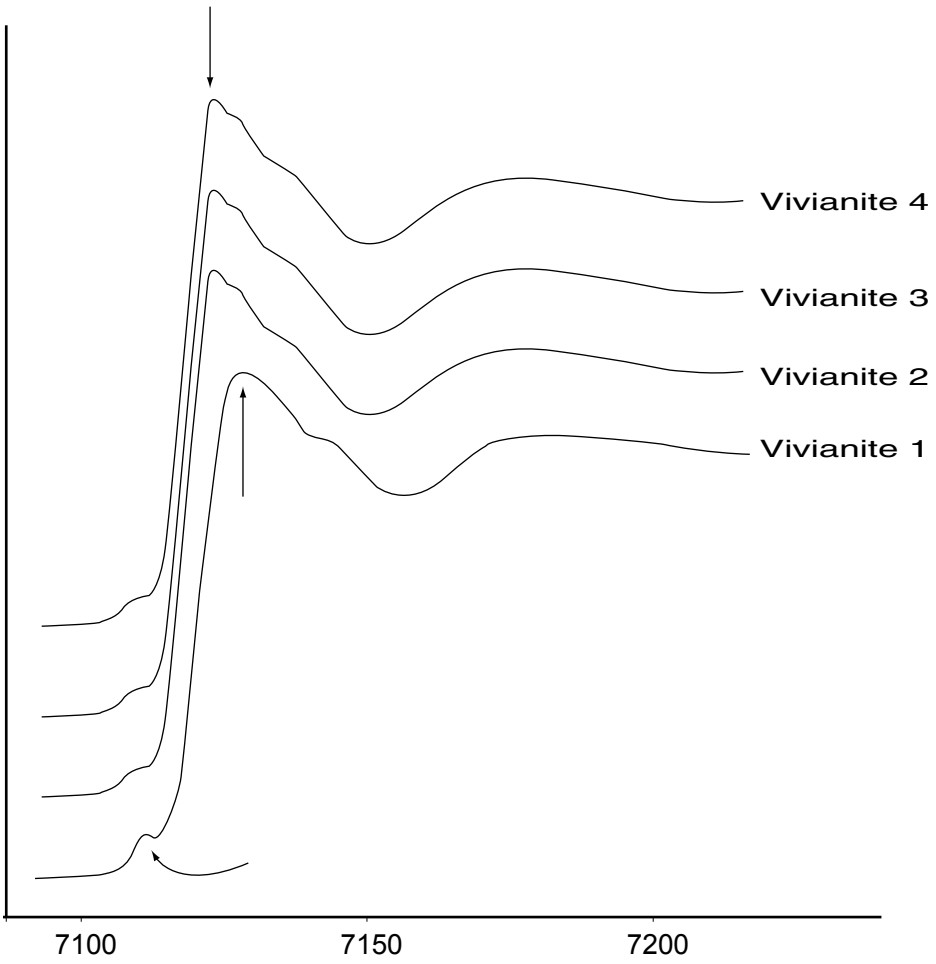
Vivianite 4
Vivianite 3
Vivianite 2
Vivianite 1
7100
7150
7200

Vivianite 1

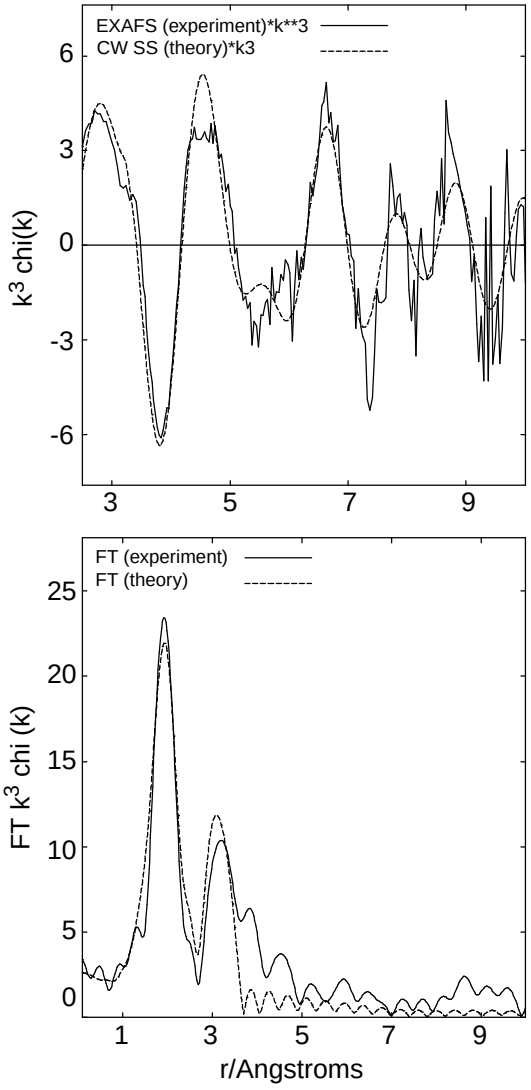

Vivianite 4

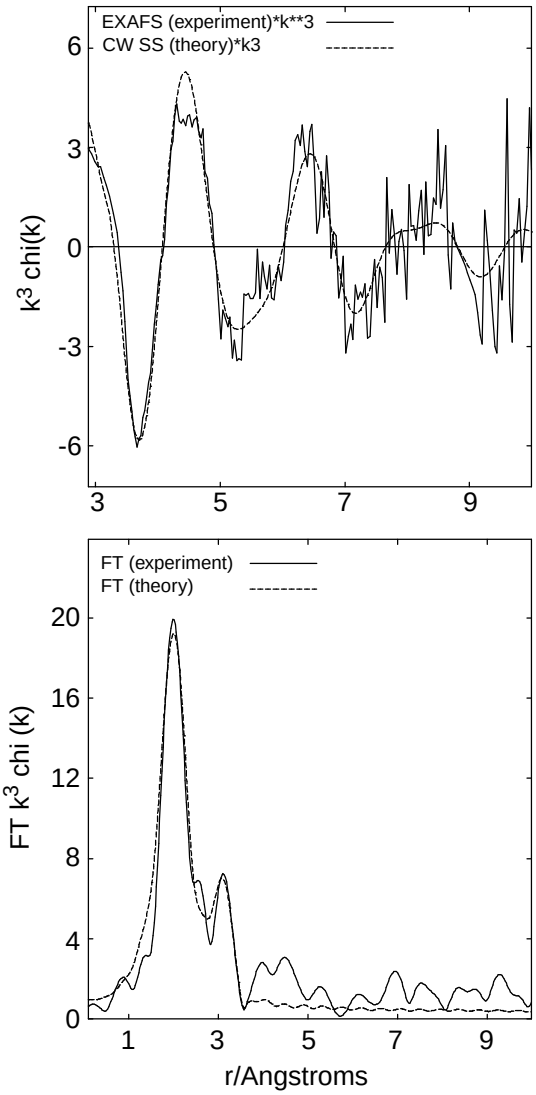

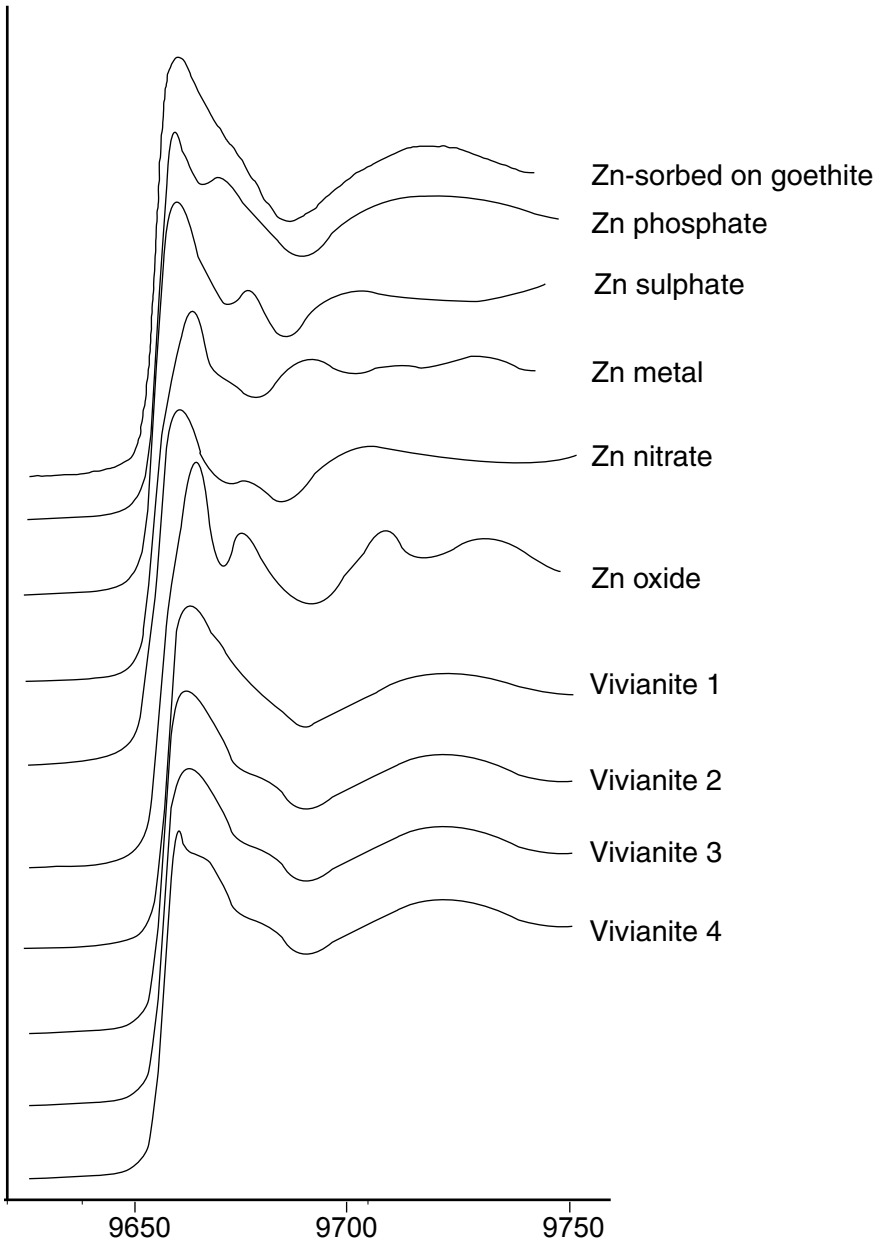
Zn-sorbed on goethite
Zn phosphate
Zn sulphate
Zn metal
Zn nitrate
Zn oxide
Vivianite 1
Vivianite 2
Vivianite 3
Vivianite 4
9650
9700
9750

Vivianite 2

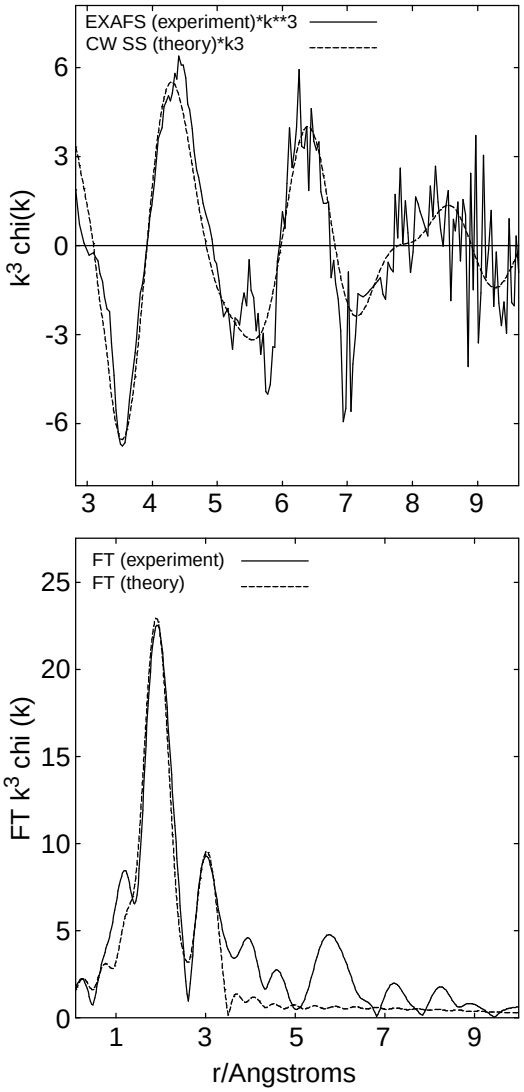

Vivianite 3

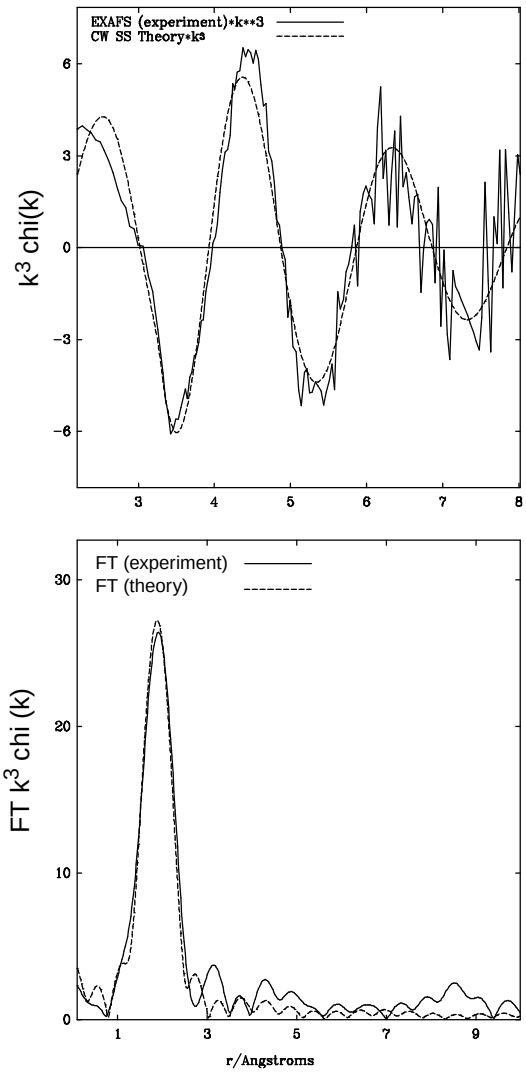

Table 1. Parameters used in fitting Fe and Zn K-edge EXAFS data for Salford Quays vivianite grains. $2\sigma^2$ is the Debye-Waller type factor, and the R factor indicates quality of fit (lower R factor indicates a better fit). Structural data of vivianite (averages) from Mori and Ito (1950), Fejdi et al. (1980) and Bartl (1989) are shown for comparison purposes. Errors in this table are as follows: Number of atoms ± 1; r ± 0.02Å; DW ± 0.002Å2.

Element	*Analysed Grain*	*Scatterer*	*No of Atoms*	*R (Å)*	*$2\sigma^2$ (Å^2)*	**R *factor***
Fe	**1**	O	4	1.99	0.031	39.73
		P	2	3.17	0.007	
	2	O	4	2.03	0.025	39.01
		P	2	3.25	0.020	
	3	O	4	2.05	0.023	48.80
		P	2	3.21	0.012	
	4	O	4	2.05	0.028	39.48
		P	2	3.23	0.027	
Zn	**1**	Not determined				
	2	O	4	1.97	0.025	41.70
		O	2	2.98	0.021	
		P	2	3.17	0.028	
	3	O	4	1.97	0.021	31.90
	4	Not determined				
Fe	**Mori and Ito, 1950**	O	2	1.98		
		O	4	2.02		
		P	2	3.28		
Fe	**Fejdi et al., 1980**	O	2	2.06		
		O	4	2.18		
		P	2	3.22		
Fe	**Bartl, 1989**	O	2	2.06		
		O	4	2.19		
		P	2	3.23		